

## Coupled Simulations of Cooling and Engine Systems for Unsteady Analysis of the Benefits of Thermal Engine Encapsulation

BLAGO MINOVSKI

Department of Applied Mechanics  
CHALMERS UNIVERSITY OF TECHNOLOGY  
Göteborg, Sweden 2015



THESIS FOR THE DEGREE OF LICENTIATE OF ENGINEERING IN MACHINE  
AND VEHICLE SYSTEMS

Coupled Simulations of Cooling and Engine Systems for  
Unsteady Analysis of the Benefits of Thermal Engine  
Encapsulation

BLAGO MINOVSKI

Department of Applied Mechanics  
CHALMERS UNIVERSITY OF TECHNOLOGY

Göteborg, Sweden 2015

Coupled Simulations of Cooling and Engine Systems for Unsteady Analysis of the Benefits  
of Thermal Engine Encapsulation  
BLAGO MINOVSKI

© BLAGO MINOVSKI, 2015

Thesis for the degree of Licentiate of Engineering 2015:07  
ISSN 1652-8565  
Department of Applied Mechanics  
Chalmers University of Technology  
SE-412 96 Göteborg  
Sweden  
Telephone: +46 (0)31-772 1000

Cover:  
Temperature field in underhood - CFD results from complete vehicle simulation

Chalmers Reproservice  
Göteborg, Sweden 2015

Coupled Simulations of Cooling and Engine Systems for Unsteady Analysis of the Benefits of Thermal Engine Encapsulation

Thesis for the degree of Licentiate of Engineering in Machine and Vehicle Systems

BLAGO MINOVSKI

Department of Applied Mechanics

Chalmers University of Technology

## ABSTRACT

A number of studies show that a well-designed engine encapsulation can extend engine cool-down time significantly - on the order of 500 - 700 percent. This is expected to have a sensitive influence on the fuel consumption due to the increased probability for high oil temperatures at the following engine start, reduced length of the initial warm-up period and consequently, reduced friction losses.

This work aims to set up and develop a simulation platform for investigations of the potential effect of thermal engine encapsulation on fuel consumption of commercial and passenger vehicles. It documents the development and validation of the methods and tools used for this purpose and applies them to estimate the effect of various initial oil temperatures on the fuel consumption of a commercial vehicle during a cold start drive cycle.

Presented is a comprehensive 1D unsteady model verified against experimental data and supported with parallel 3D simulations. The model contains predictive representations of engine, cooling system, oil circuit and utilizes a temperature dependent model of engine friction losses. A number of steady-state and transient simulations are performed for a 13L Volvo FM commercial vehicle and results are compared with physical measurements. The developed 1D and 3D methodologies were validated and achieved satisfactory accuracy both in steady and unsteady mode of operation. Predictions of oil sump temperature development were compared to measured values to conclude that the model is fit for further use in a temperature dependent friction model.

As a last step all models were unified to perform a complete vehicle simulation of a cold start drive cycle at different initial oil temperatures in order to evaluate the influence of reduced warm-up phase on fuel consumption. The simulations indicated that there is a potential for up to approx. 3% decrease of fuel consumption as a result of increased initial engine temperatures.

Keywords: 1D simulations, CFD simulations, Fuel consumption, Drive cycle, Cooling system, Oil system, Engine encapsulation

## ACKNOWLEDGEMENTS

I would like to express my sincere gratitude to those, who made this work possible and who helped me during my study.

First of all I would like to thank my supervisors Ph.D Peter Gullberg and Professor Lennart Löfdahl for guiding and supporting me through all stages of my work, securing necessary connections and resources within the organizations, for their trust and vision. Furthermore I would also like to acknowledge with much appreciation the manager of Simulation & Testing group and official manager of this project Peter Nillsson, who ensured a good environment for my work.

I would like to thank all specialists at Volvo Trucks, who supported this project: Torbjörn Wiklund and Sassan Etemad for their great help with CFD simulations, Elias Johansson for his valuable help with setting up the engine model, Christoffer Bäckvall for his help with the fan control software, Stina Karlsson, Anna Rimark, who provided me with useful data for the coolant pump and coolant circuit, Anders Ottosson and Björn Andre for their advice regarding physical testing and Dennis Engberg, who solved many of my IT issues.

This project would not be possible without the funding provided by the Swedish Energy Agency within the framework *Strategic Vehicle Research and Innovation*.

Last, but not least I would like to thank all members of this project's Steering Committee for their thoughtful attitude and valuable advice: Lennart Löfdahl, Peter Nilsson, Kjell Andersson from Volvo GTT, Alexander Broniewicz, Jerry Sjösten, Mats Löfman from Volvo Cars Corporation and Per Jonsson and Mattias Chevalier from Scania.

## NOMENCLATURE

$\sigma$	Stefan-Boltzmann constant	$\left[\frac{W}{m^2 K^4}\right]$
$\varepsilon$	Emissivity	$[-]$
$\rho$	Density	$\left[\frac{kg}{m^3}\right]$
$\mu$	Dynamic viscosity	$\left[\frac{kg}{sm}\right]$
$A$	Flow area	$[m^2]$
$A_s$	Heat transfer surface area	$[m^2]$
$C_f$	Skin friction coefficient	$[-]$
$H$	Total enthalpy	$\left[\frac{J}{kg}\right]$
$K_p$	Pressure loss coefficient	$[-]$
$R$	Ideal gas constant	$\left[\frac{J}{kgK}\right]$
$V$	Volume	$[m^3]$
$e$	Total internal energy	$\left[\frac{J}{kg}\right]$
$h$	Convective heat transfer coefficient	$\left[\frac{W}{m^2 K}\right]$
$k$	Thermal conductivity	$\left[\frac{W}{m^2 K}\right]$
$m$	Mass contained in a volume	$[kg]$
$p$	Pressure	$[Pa]$
$q$	Heat flux density	$\left[\frac{W}{m^2}\right]$
$u$	Internal energy	$\left[\frac{J}{kg}\right]$
$v$	Velocity	$\left[\frac{m}{s}\right]$

## ABBREVIATIONS

1D	One-dimensional
3D	Three-dimensional
CAC	Charge air cooler
CAD	Computer aided design
CFD	Computational fluid dynamics
CO	Carbon monoxide
DNS	Direct numeric simulations
ECU	Engine control unit
EMS	Engine management system
FMEP	Friction mean effective pressure
HC	Hydrocarbons
ICE	Internal combustion engine
IMEP	Indicated mean effective pressure
LES	Large eddy simulations
MRF	Moving reference frame
NEDC	New European drive cycle
NO <sub>x</sub>	Nitrous oxide
OAPEC	Organization of Arab petroleum export countries
PM	Particulate matter
RANS	Reynolds-averaged Navier-Stokes
RT	Real time
VS	Virtual section

# THESIS

This thesis consists of an extended summary and the following appended papers:

- Paper A** Minovski, B. and Lofdahl, L., "Study of Software Integration for Transient Simulation of Future Cooling System for Heavy Truck Application," SAE Technical Paper 2014-01-0653, 2014, doi:10.4271/2014-01-0653.
- Paper B** Minovski, B., Lofdahl, L. and Gullberg, P., "A 1D Method for Transient Simulations of Cooling Systems with Non-Uniform Temperature and Flow Boundaries Extracted from a 3D CFD Solution," SAE Technical Paper 2015-01-0337, 2015, doi:10.4271/2015-01-0337.



# CONTENTS

<b>Abstract</b>	<b>i</b>
<b>Acknowledgements</b>	<b>ii</b>
<b>Nomenclature</b>	<b>iii</b>
<b>Abbreviations</b>	<b>iv</b>
<b>Thesis</b>	<b>v</b>
<b>Contents</b>	<b>vii</b>
<b>1 Introduction</b>	<b>1</b>
1.1 Background . . . . .	1
1.2 Motivation . . . . .	1
1.2.1 Emissions and environment . . . . .	1
1.2.2 Price of fuel . . . . .	2
1.3 Purpose . . . . .	3
1.4 Limitations . . . . .	4
<b>2 Theory</b>	<b>5</b>
2.1 Importance of engine cooling . . . . .	5
2.2 Modes of heat transfer . . . . .	5
2.2.1 Conduction . . . . .	5
2.2.2 Convection . . . . .	6
2.2.3 Radiation . . . . .	6
2.3 The automotive cooling system . . . . .	7
2.3.1 Cooling system components . . . . .	8
2.3.2 The automotive lubricating system . . . . .	11
2.3.3 Engine encapsulation . . . . .	11
2.3.4 Numerical expressions . . . . .	12
<b>3 Method</b>	<b>14</b>
3.1 Physical measurements . . . . .	14
3.2 Simulation models . . . . .	15
3.2.1 1D simulation models . . . . .	15
3.2.2 3D simulation models . . . . .	19
3.2.3 Imposing results from 3D CFD to 1D models . . . . .	20

<b>4 Results</b>	<b>22</b>
4.1 Results from basic 1D model . . . . .	22
4.1.1 Steady state simulations . . . . .	22
4.1.2 Continuous transient drive cycle simulations . . . . .	23
4.2 Results from 3D simulations of complete vehicle . . . . .	25
4.3 Results from a 1D model with non-uniform boundary conditions with input from 3D simulations . . . . .	27
4.4 Unsteady simulations of engine cold start and predictions of fuel consumption	28
<b>5 Conclusions</b>	<b>33</b>
<b>6 Future work</b>	<b>34</b>
<b>References</b>	<b>35</b>
<b>Paper A</b>	<b>37</b>
<b>Paper B</b>	<b>51</b>

# 1 Introduction

This chapter contains the reasons and motivations for starting the project and explains its relevance. The project goals are also outlined.

## 1.1 Background

Contemporary automotive industry is constantly challenged by fierce technological competition motivated by increasing customer demands and most importantly, continuously growing criteria for overall energy efficiency and reduction of CO<sub>2</sub> emissions. In order to satisfy these tough requirements automotive designers constantly seek to improve the functionality of every single automotive system and component and optimize it in terms of their influence on the overall fuel consumption and emissions of the vehicle.

Despite the long history of automotive development, since its beginning in the second half of 19-th century, the thermodynamic efficiency of a modern diesel engine used in a commercial vehicle does not exceed 40 percent. One way to improve the efficiency is by minimizing the friction losses [7] (due to high viscosity of the cold engine oil during startup) by introducing an encapsulation of the engine, which would act as a thermal barrier between the engine and the environment and would therefore increase the probability that the engine oil temperature would be high during the following engine start.

## 1.2 Motivation

### 1.2.1 Emissions and environment

The scale and dynamics of contemporary industrial and economic development would not be possible without effective logistic networks and rapid transportation. With this in mind it is not surprising that the transport sector is the largest end-user source sector of CO<sub>2</sub> emissions. Energy consumption and emissions from transport are dominated by oil usage for road transport with an average annual increase of 1.7% since year 2000. [17] In an attempt to control emissions from the automotive industry, the European Union introduced a system of regulating limits for some of the most harmful substances released into the atmosphere as a result of internal combustion engine operation. The first enforcement of these rules was done in the early 1990's with the introduction of Euro 1. Vehicles which did not pass the specifications prescribed in this standard, after being tested with a standardized test cycle, were not to be allowed on the European market. Target emissions regulated by this standardization system include carbon monoxide (CO), nitrous oxide (NO<sub>x</sub>), hydrocarbons (HC), and particulate matter (PM). Over the following decades until present time the European emission standard system has been successively updated and emission levels have been significantly reduced, thus stimulating car makers to invest in new technologies for cleaner and more energy efficient automotive systems.

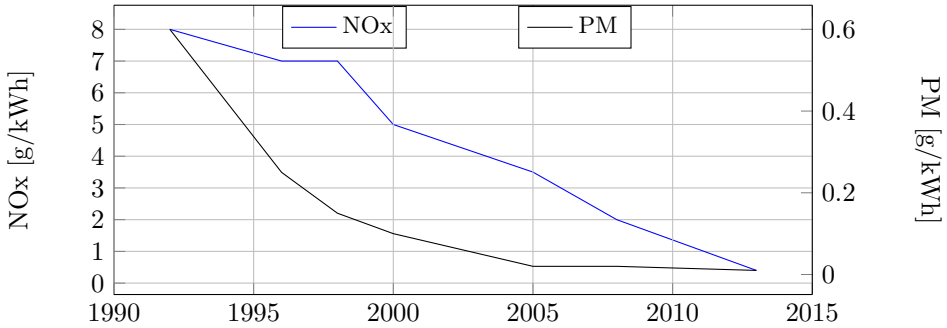


Figure 1.1: *Limits for heavy duty diesel engines - European emission standard*

### 1.2.2 Price of fuel

After the advent of ICE engines in the end of 19-th century, coal ceased to be the major global energy source and was surpassed by oil, which takes the largest share of fuels used today. It is estimated that since 1965 between 100 and 135 billion tonnes of oil has been consumed [16]. Such an amount of crude oil would fit in a hypothetical cubic tank with an edge of 5.5 kilometers. If its height would be 1 meter, then the tank would spread over a third of Sweden's territory.

For a number of decades now there has been an escalating environmental and strategic

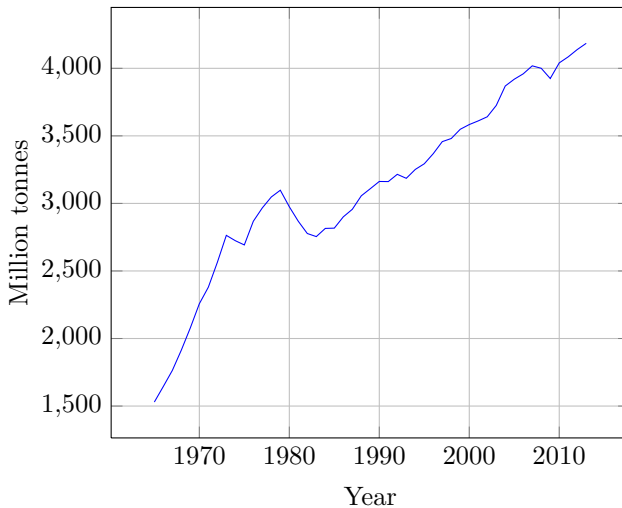


Figure 1.2: *Global oil consumption*

concern regarding the non-sustainable transport sector of today, primarily powered by oil. As with any other commodity, price of oil is also governed by principles of supply and demand, Figures 1.2 and 1.3. Figure 1.4 presents a combined plot where one can observe the inter-dependability of oil production and price. With vigorous development of

automobilization worldwide in the early 1970's oil supply increases linearly, until October 1975 when OAPEC started an oil embargo, which resulted in the first oil crisis and 200% increase in price, followed by the second oil crisis in 1979, after which oil prices skyrocketed to over 100 dollars per barrel to reach pre-crisis levels again in the late 90's. Recent massive economic growth in developing countries imposes increasing energy demands, that have resulted in a steady oil price growth hitting record levels in 2013. Despite the most recent dip in oil prices during 2014 and 2015, it is obvious that global energy demands are becoming bigger and it is reasonable to expect that prices in the long run will eventually increase.

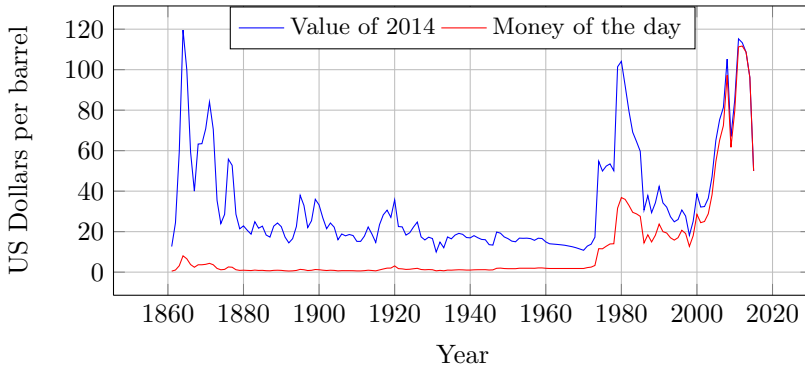


Figure 1.3: *Development of oil price*

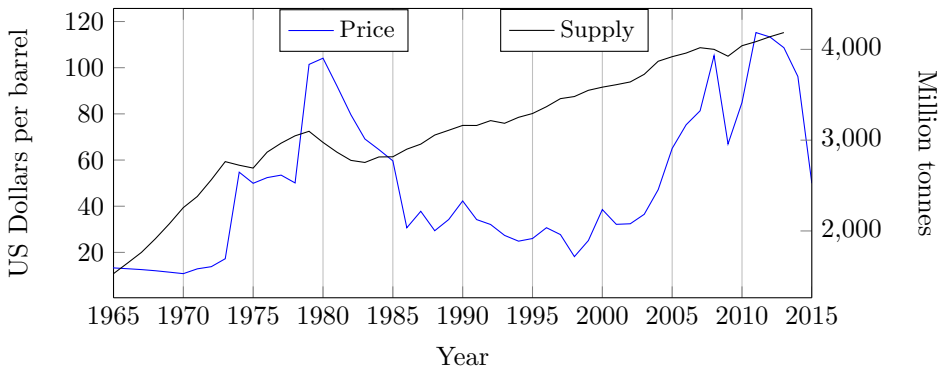


Figure 1.4: *Development of oil price and production*

### 1.3 Purpose

This project aims to construct and validate a simulation platform for modeling and quantifying energy transfer between engine, cooling and oil systems for accurate prediction

of coolant and oil temperatures and their effects on the overall energy efficiency of the vehicle.

The knowledge within method development and validation from this and future related works can be supplemental in investigations of unsteady thermal radiation effects in engine bay - thermal soak, hot spots and also for studies of energy recovery strategies.

## **1.4 Limitations**

The system delivered as a result from this work is seen as a foundation and a unifying platform of a number of tools and methods for analysis of thermal engine encapsulation and its effects on fuel consumption, emissions and noise. The presented approach is mainly one-dimensional and it investigates the effects of different initial oil sump temperatures on the fuel consumption during the warm-up period.

However, a three-dimensional method is investigated and intended as an add-on to the main platform. Additional 3D methods for different types of analysis, e.g. natural convection in the engine bay, etc. are planned for development in near future.

## 2 Theory

### 2.1 Importance of engine cooling

There are many streams of energy transfer in a common automotive system, which could be examined from many angles, but they all source from the work produced by burning fluids in the combustion chamber of the engine. During this process peak burned gas temperatures of up to 2500 K are reached. However the maximum allowed temperatures for components in the combustion chamber are significantly lower, therefore cooling of the cylinder liners, piston, ect. must be provided. High temperature gradients in the combustion chamber and high local gas velocities inside it result in high heat fluxes [11]. In areas of high heat fluxes thermal stresses must be kept low in order to avoid cracks. The inside wall of the cylinder liner and combustion chamber must be regulated below 180 C° in order to prevent deterioration of the lubricating oil film.

Furthermore, heat transfer rates from the burned gas to the engine components affect thermal efficiency, emissions and lifetime of the engine. High rates of heat transfer to the components of the combustion chamber reduce the average gas temperatures and consequently reduce the work extracted from the gas expansion during the working cycle. The cooling capacity exerted on the cylinder liners affects the gas-side surface temperature and consequently the oil film viscosity which has a direct influence on the piston-to-cylinder friction and the overall engine friction losses. This illustrates the importance and necessity of engine cooling. [6]

### 2.2 Modes of heat transfer

#### 2.2.1 Conduction

Conduction is a heat transfer mechanism, where energy is transmitted by microscopic diffusion and collision of particles within a body as a result from a temperature gradient. Conduction occurs in solids, liquids, gases and plasmas. In the absence of any external drives conduction will work to reduce the temperature gradient. The magnitude of the transferred heat is proportional to the temperature gradient and hence the heat flux  $\dot{q}$ , can be described by equation 2.1

$$q_i = -k \frac{\partial T}{\partial x_i} \quad (2.1)$$

A good example of a cooling system component, where pure conduction takes place, is the wall of any heat exchanger, across which thermal energy is transferred from one media to another without mixing. The heat transfer through the material of the wall is driven by conduction.

## 2.2.2 Convection

Convection is a mechanism of heat transfer, where physical movement of a medium facilitates the transfer of thermal energy. It is the most common heat transfer mode in fluids and it is said to comprise of heat diffusion (conduction) and heat transfer by bulk fluid flow, known as advection [3]. Convection can be forced - when the movement of the medium is caused by an external drive, or natural - when fluid buoyancy is the only driving force for the motion of the surrounding fluid.

In a cooling system, convection occurs on both sides of any heat exchanger and in the coolant circuit itself. With prospect of increasing the efficiency of the energy transfer, convection in cooling systems is most often forced by a pump or a fan. Equation 2.2 provides a mathematical expression for the convective heat flux.

$$\dot{q} = h(T - T_w) \quad (2.2)$$

## 2.2.3 Radiation

All matter, that has temperature greater than the absolute zero emits energy in the form of electromagnetic waves. In this context radiation can be seen as a conversion of thermal energy into electromagnetic energy as a result of the oscillation of the micro-particles in matter and the consequent generation of coupled electric and magnetic fields, which emit photons and radiate energy away from the body through its surface. Radiation is a heat transfer mechanism, which does not require the presence of a medium and radiative heat propagates with the speed of light infinitely far unless obstructed.

The intensity of the transmitted radiative heat emitted by a surface of a black body is proportional to the fourth power of its absolute surface temperature. This relationship is defined by the Stefan-Boltzmann law in equation 2.3

$$E_{rad} = \sigma T_s^4 \quad (2.3)$$

where  $\sigma$  is the Stefan-Boltzmann constant,  $5.6704 \times 10^{-8} \left[ \frac{W}{m^2 K^4} \right]$  and  $T_s$  is the absolute temperature of the surface [K].

Generally a body emits only a portion of the energy stated in the ideal case of a black body from equation 2.3. For this reason a non-dimensional coefficient of thermal emissivity,  $\varepsilon$  in the range  $0 < \varepsilon < 1$  is introduced as follows:

$$E_{rad} = \varepsilon \sigma T_s^4 \quad (2.4)$$

The net radiative heat flux is given in equation 2.5

$$\dot{q}_{rad} = \varepsilon \sigma (T_s^4 - T_\infty^4) \quad (2.5)$$

where  $T_\infty$  is the temperature of the surrounding environment.

## 2.3 The automotive cooling system

The main purpose of a cooling system as a part of an internal combustion engine is to reject heat from the engine block and other engine peripherals to the environment and thus maintain an optimal temperature of operation. Heywood [6] points out, that in modern diesel engines the cooling system rejects within the range of 16 to 35 % of the fuel heating value depending on the engine's construction and mode of operation.

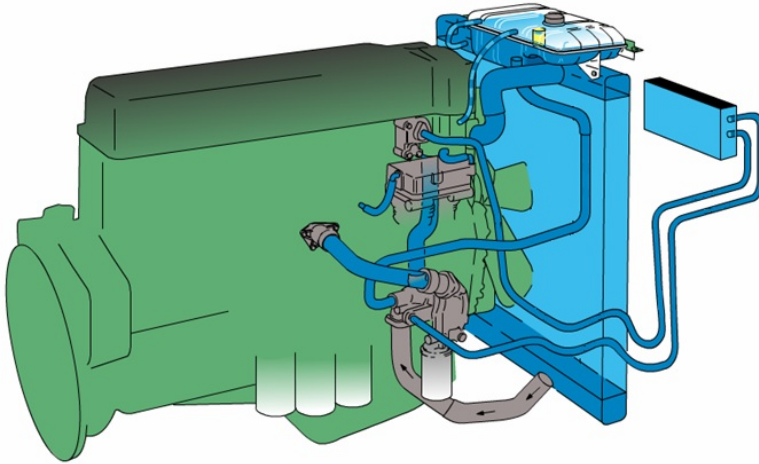


Figure 2.1: *Cooling system of a truck*

A schematic of a basic truck cooling system is shown on figure 2.2. It presents a cooling package consisting of a charge air cooler (CAC), radiator and a fan.

To perform its function the cooling system needs a thermal interface with the surroundings, which is most effectively provided by heat exchangers. However, heat transfer occurs not only through them, but also through the walls of the coolant transportation system (pipes and hoses) as well as through other components including the engine block itself by a combination of convection and radiation.

Practically all the parts of the cooling circuit take part in some form of heat transfer and in other phenomena, which have a direct influence on it (f.ex. pressure drops influence fluid flow rate, which determines the convective heat transfer coefficient). Therefore, there are many physical phenomena one could model in order to capture the system behavior most thoroughly.

Under normal operating conditions the coolant temperature would be maintained below  $105\text{ }^{\circ}\text{C}$ . The most direct mechanism to control the coolant temperature is by adjusting the speed of the fan, which is of suction impeller type. As in most automotive cooling systems the thermostatic valve ensures quick arrival at operating temperatures and it is one of the thermal controls on the liquid side together with the coolant pump control. The following subsections give a short account for each basic component in the cooling system.

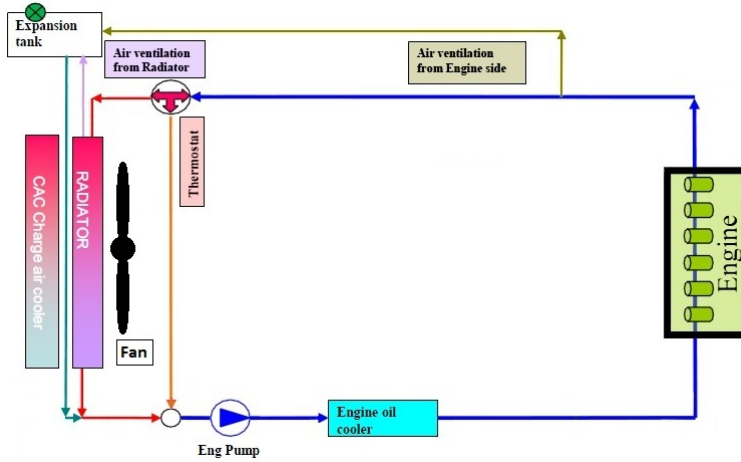


Figure 2.2: *Schematic of a truck's cooling system (basic components)*

### 2.3.1 Cooling system components

Depending on the specific vehicle setup there may be a number of different heat exchangers present in a water-cooler engine installation. Apart from the necessary radiator, which serves as the main thermal interface between the hot engine coolant and the environment, the cooling package may include a series of other heat exchangers. Most contemporary diesels, for example are fitted with a charge-air-cooler (CAC), whose function is to cool down the hot compressed air after the turbo-compressor or supercharger. In most cases it is air-to-air heat exchanger mounted directly before the radiator in the cooling stack, where it operates at close to ambient temperatures. When a low-temperature cooling circuit is available a water cooled CAC may be used, which is a water-to-air heat exchanger. The condenser radiator is typically mounted before the CAC in the heat exchanger stack and it is a part of the truck's climate control system.

The internal medium of the condenser is refrigerant. It enters the condenser downstream of the climate compressor as superheated gas. As it travels through the tubes of the condenser it rejects heat. During this process the internal energy of the superheated refrigerant decreases until it condenses into liquid phase.

As this work assumes pre-defined constant heat addition from the condenser (typically zero for most test drive cycles), it does not attempt to model and simulate the heat transfer between the refrigerant and the environment. Therefore multiphase heat transfer will not be modeled, but the condenser radiator will be present in the model of the air path with its pressure loss characteristics and constant pre-defined heat addition.

Efficient heat transfer on the liquid side of any modern water cooled automotive cooling system occurs thanks to forced convection. The main drive of this phenomenon is the pressure rise (head) created by the coolant pump, which leads to coolant circulation. Most automotive coolant pumps are of centrifugal type, located on the low-temperature side of the coolant circuit downstream the radiator. The coolant pump is usually permanently

coupled to the crankshaft by some type of torque transfer arrangement: a belt or a gear drive, which imposes a fixed gear ratio. For reasons related to fuel efficiency some modern automotive coolant pumps are coupled to the drive by an electromagnetic or viscous clutch. This flexible control allows to interrupt the direct connection of the pump impeller to the pump input shaft and reduce the speed of the impeller in relation to the engine speed, which consequently reduces the energy consumption of this auxiliary component. A control strategy implemented in the ECU activates the clutch depending on parameters as coolant temperature, engine torque, engine speed, etc.

Coolant mixture is circulated through the coolant circuit into the engine block and its cooling channels, through the channels in the cylinder head and through all other heat exchanges connected to the liquid side of the system. It is the main internal medium for heat transportation. In most automotive applications the coolant mixture consists of water, ethylene glycol and other additives mixed in a certain proportion.

The thermostat is a controllable valve, which can be adjusted to bypass coolant flow away from the radiator through a parallel line in order to faster reach and maintain the recommended temperature range for engine operation. Most automotive thermostatic valves are controlled by an in-built thermo-sensitive wax-filled mechanical actuator.

The radiator's external coefficient of heat transfer changes with the amount of air flowing through its core. As the vehicle moves forward, static pressure builds up in front of the radiator generating a natural flow through the core referred to as ram air effect. This is, however not sufficient for all operating ranges of the engine and it is therefore necessary to provide a mechanism, which would drive extra air mass through. This is done by the cooling fan, which is most commonly of axial impeller type with a shroud in order to ensure relatively even mass flow through the entire surface of the core.

Cooling is a major function of engine oil. As it travels through the oil channels in the engine block and as it cools down the piston-cylinder assembly it receives heat, which must be rejected. This is done through a dedicated heat exchanger referred to as engine oil cooler.

## **Recirculation**

Hot air recirculation is a phenomenon, which occurs in the engine bay and its surroundings. It is driven by the increased pressure in the regions after the fan. Under different operating conditions some quantities of hot air from this high pressure region may be pulled towards regions of lower pressure levels in front of the radiator, CAC and in front of the entire cooling package. A principle representation of the phenomenon is shown on Figure 2.3

The effect of hot air recirculation can be best modeled by 3D CFD tools. In fast running 1D simulation it is represented by a simplified model usually including preheating of the inlet ram air by a heat addition object or by simply imposing a certain increase in ambient temperature. Magnitudes of ambient air temperature increase for compensating the effect of hot air recirculation are usually acquired from test and calibration for steady state mode of operation.

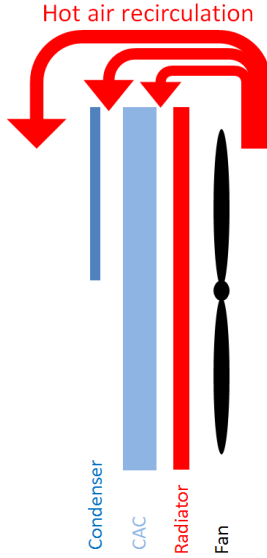


Figure 2.3: *Effect of hot air recirculation*

## Nonuniformity

In a stacked cooling package the heat transfer through each heat exchanger depends on the mass flows and temperature distribution [8]. Due to the high levels of turbulence in a typical installation operating at high fan speeds the temperature and flow fields at the inlets of the heat exchangers are greatly affected by the complex three-dimensional unsteady nature of the turbulent flow in the underhood and are inherently non-uniform. Such non-uniformities are reported to decrease the effectiveness of the heat exchangers and it is suggested that the accuracy of analysis may be improved if the effect of non-uniform velocity and mass flow distribution is captured in the simulation. Velocity non-uniformity can be quantified and measured by the so called non-uniformity index defined as follows:

$$i = \frac{1}{n} \sum_{K=0}^n \frac{|\dot{m}_K \frac{A_R}{A_K} - \dot{m}_{tot}|}{\dot{m}_{tot}} \quad (2.6)$$

where

$\dot{m}_K$  - mass flow through one area section

$A_K$  - size of one area section

$\dot{m}_{tot}$  - total mass flow

$A_R$  - face area of core

$A_{ref}$  - area of corresponding section

An increasing non-uniformity index indicates less uniform distribution.

### 2.3.2 The automotive lubricating system

Not all the work exerted on the pistons by the burned air-fuel mixture is available at the driveshaft for actual use. A significant part of it is transformed in different ways within the engine system and finally dissipated as heat into the coolant or oil. One major function of the lubricating system is to absorb and transport this friction heat away. Naturally the viscosity of oil, which is specific for each lubricant and greatly depends on temperature, has a substantial influence on the friction losses, which occur in the engine. A cold engine contains oil of high viscosity, which is energetically more expensive to agitate compared to a hot, engine, whose oil is thin. This is a motivation for having a thermostatic valve on the oil circuit for heavy-duty applications. Fuel efficiency during the warm-up phase is improved by ensuring a quick arrival at nominal oil working temperature by temporarily bypassing the oil cooler during the period of time when engine oil is cold, which amounts to up to 20-25 minutes for a middle sized commercial distribution vehicle.

### 2.3.3 Engine encapsulation

The idea of partly or fully enclosing the engine by an isolating structure in order to minimize heat dissipation and noise propagation to the surroundings is not new, but became popular and interesting to automotive research due to the increasingly tough requirements for efficiency and growing environmental concerns. Numerous researches on the topic [12], [19], [18], report that it is possible to significantly improve both engine efficiency and reduce noise emissions by a clever encapsulation concept at an acceptable cost.

#### Types and expected effects

Engine encapsulations could be classified in terms of their application and implementation. There are two main reasons, which separately or together may motivate the use of engine encapsulation: to reduce heat losses and noise emissions. Nevertheless any structure introduced in the engine bay with either purpose will have an effect on both thermal and acoustic phenomena. This motivates to adapt the design process by considering both phenomena and take full advantage of the structure. Depending on the implementation encapsulations can be engine-mounted when they are located in direct proximity to the engine block, or encapsulating the entire engine bay including other components of the engine installation [19]. From a thermal management perspective the main advantage of the engine encapsulation is that it reduces the amount of heat transfer from the hot engine to the cold ambient air particularly in the periods of time when the engine is still warm and has just been switched off. The reduced convective cooling achieved by the encapsulating structure increase the cool-down time of the engine fluids and consequently increase the probability of hot oil temperatures at the following engine start. In this relation Rieter [12] claim that a reduction of up to 2.7% in  $CO_2$  emissions is achieved for a 1.9L Diesel engine during NEDC as a result of a complete engine encapsulation. A 9.4 K of temperature increase to baseline vehicle is reported after 12h cool-down period at an ambient of 10 C° at the cost of 7.5 kg increase in weight.

### 2.3.4 Numerical expressions

This section briefly summarizes the fundamental fluid mechanics theory used in the one and three-dimensional modeling methods employed in this work. Both 1 and 3D tools employ the principles of continuity, conservation of mass and energy equations. However, their implementation differs.

The flow model involves the solution of the Navier-Stokes equations, namely the conservation of continuity, momentum and energy equations:

$$\frac{dp}{dt} + \rho \frac{\partial v_i}{\partial x_i} = 0 \quad (2.7)$$

$$\rho \frac{dv_i}{dt} = -\frac{\partial p}{\partial x_i} + \frac{\partial \tau_{ji}}{\partial x_j} + \rho f_i \quad (2.8)$$

$$\rho \frac{de}{dt} = \tau_{ji} \frac{\partial v_i}{\partial x_j} - p \frac{\partial v_i}{\partial x_i} - \frac{\partial q_i}{\partial x_i} + \rho v_i f_i \quad (2.9)$$

These are nonlinear partial differential equations and when applied for large-volume systems certain terms in them must be modeled.

Density and its variation with pressure and temperature is captured by the ideal gas law:

$$\rho = \frac{p}{RT} \quad (2.10)$$

The viscous stress term for Newtonian fluids, used in the momentum and energy equations is defined as:

$$\tau_{ij} = 2\mu \left( \frac{1}{2} \left( \frac{\partial v_i}{\partial x_j} + \frac{\partial v_j}{\partial x_i} \right) - \frac{1}{3} \frac{\partial v_k}{\partial x_k} \delta_{ij} \right) \quad (2.11)$$

The heat flux used in the energy equation is defined by the Fourier's law (constitutive law for heat flux vector), equation 2.1.

Different methods to implement and solve the above relationships can be employed depending on the specific situation concerned: Reynold's Averaged Navier Stokes (RANS) simulations, Large-Eddy-Simulations (LES), Direct Numerical Simulations (DNS), etc.

The Navier-Stokes equations can be modeled with Reynold's decomposition where the transport variables are presented as a sum of a time-averaged part and instantaneous fluctuation:

$$\begin{aligned} v_i &= \bar{v}_i + v'_i \\ p_i &= \bar{p} + p'_i \end{aligned}$$

After substitution in equation 2.8 a non-linear term is left  $\overline{\rho v'_j v'_i}$  known as the Reynold's stresses. A turbulence model is required to estimate this term. Different models may be applied for this purpose. Most frequent RANS turbulent models are Eddy Viscosity model and the Reynold's stress transport model [1]. A subset of the Eddy Viscosity models, which employ the Boussinesq assumption are the so called Two-Equation models, which

introduce two additional transport equations that represent the turbulent properties of the flow. Such Two-Equation models are for example the standard  $k - \varepsilon$ , the realizable  $k - \varepsilon$  and the  $k - \omega$  models, where  $k$  is the turbulent kinetic energy,  $\varepsilon$  is the turbulent dissipation and  $\omega$  is the specific dissipation.

For one-dimensional analysis governing equations are still the Navier-Stokes equations, which are adapted for 1D setup:

$$\frac{dm}{dt} = \sum_{boundaries} \dot{m} \quad (2.12)$$

$$\frac{d\dot{m}}{dt} = \frac{dpA + \sum_{boundaries} \dot{m}u - 4C_f \frac{\rho v |v|}{2} \frac{dxA}{D} - K_p \left( \frac{1}{2} \rho v |v| \right) A}{dx} \quad (2.13)$$

$$\frac{d(me)}{dt} = -p \frac{dV}{dt} + \sum_{boundaries} (\dot{m}H) - hA_s(T_{fluid} - T_{wall}) \quad (2.14)$$

# 3 Method

The works presented in this summary employ one and three-dimensional CFD modeling approaches based on the Finite Volume Method to solve the Navier-Stokes equations presented in chapter 2. All simulation methods are validated by comparison with results from physical measurements performed in a climatic wind tunnel equipped with chassis dyno. This chapter provides an overview of the testing and simulation methods used.

## 3.1 Physical measurements

A number of complete vehicle drive cycle replications were performed in a climatic wind tunnel. Available are comprehensive measurements of various temperature, pressure and flow quantities in the cooling system, engine and underhood. Temperatures and flows on all sides of the heat exchangers are logged continuously during steady state and transient driving scenarios. Key performance parameters such as engine torque, speed and vehicle speed are also logged. Continuous runs of driving cycle "Hamburg-Kassel hills" are reproduced at constant preset ambient temperatures. In such a test the vehicle's driving wheels are in contact with a chassis dyno, which can be adjusted to provide a desired level of resistance regulated by a control system continuously during the test as dictated by the pre-defined drive cycle. The vehicle's accelerator pedal is continuously depressed by a trained operator in order to satisfy the torque demand. Meanwhile, the climatic equipment generates ram air corresponding to the vehicle's driving speed at the desired temperature level. The test facility allows for an authentic replication of complete continuous, unsteady drive cycles, including cold-start tests but also for steady-state simulations.

Steady-state measurements are performed at a variety of driving speeds, fan speeds and heat release rates from the cooling system to the environment.

Figure 3.1 shows torque and speed variation during a drive cycle test replica of "Hamburg-Kassel hills".

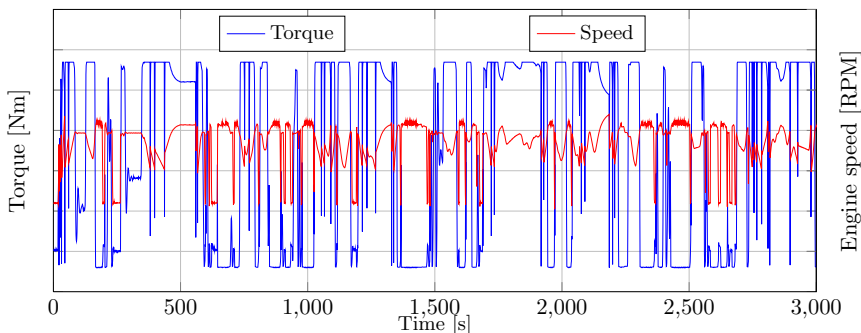


Figure 3.1: *Plot: Measured engine speed and torque during "Hamburg-Kassel hills" drive cycle*

## 3.2 Simulation models

Accurate and reliable models of energy transfer in the engine installation systems and the underhood are needed in order to predict and quantify the effects of different hardware configurations on the energy balance, fuel efficiency and emissions. A major intention with this work is to provide and validate a simulation platform capable of estimating the effects of thermal engine encapsulation concepts on the overall energy efficiency of the vehicle. This will be done by an integration of a number of 1D and 3D simulation tools. Figure 3.2 presents a schematic of the configuration.

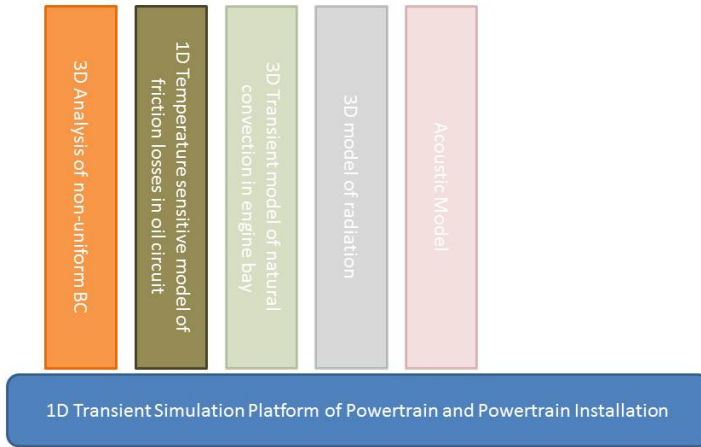


Figure 3.2: *System architecture*

A fast running 1D simulation platform including a complete powertrain model with transient drive cycle simulation capability will unify inputs provided by a number of detailed 3D and 1D models. This mechanism of model coupling will preserve the level of detail of critical intrinsically three-dimensional phenomena like turbulence and natural convection and at the same time will provide a method to utilize the outputs of these detailed models in a practical, fast running model for drive cycle simulations.

### 3.2.1 1D simulation models

#### Basic models

Provided and validated are 1D coupled models of cooling system and engine built in GT-SUITE, which is a powerful tool for modeling the fluid-dynamics and heat-transfer phenomena in the cooling system. The work includes a detailed model of the main coolant and oil circuits since this is vital for the authenticity of the transient simulation. As a first step, all necessary models and control algorithms were obtained from different technical units within the organization and were further refined to fit the purpose of this work.

Component performance data was as well acquired for different parts within the coolant and oil circuits: thermostat valves, coolant and oil pumps, engine oil cooler, etc. The system consists of two main models: engine model and a model of the cooling and oil systems, which can function independently from each other. An important feature of the interface between the engine and cooling system models, whose outline is shown on figure 3.3, is that it provides double-directional connectivity between the engine and cooling system models, enabling torque feedback from auxiliary devices like coolant pump and cooling fan to be sent back to the engine model and imposed as additional load on the crankshaft. This allows to track the influence of auxiliary power losses on the fuel consumption in a continuous drive cycle.

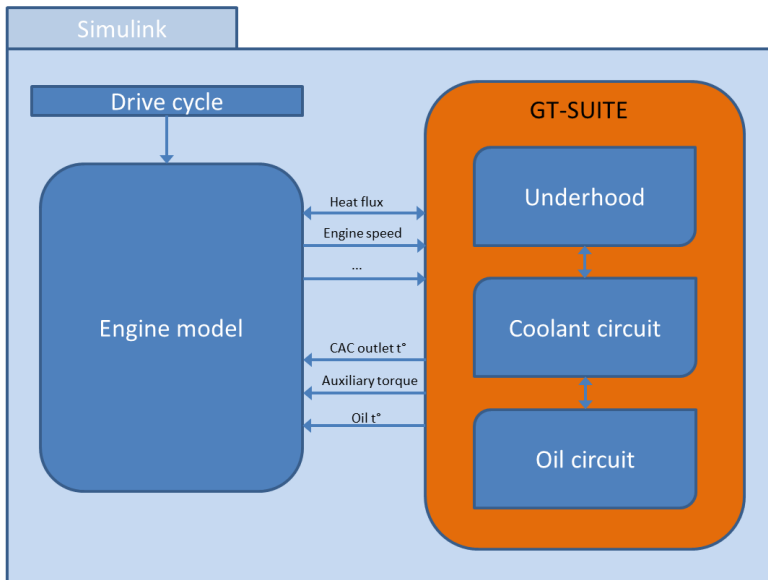


Figure 3.3: *Block diagram of powertrain and cooling system models*

The systems to be modeled are discretized into many flow volumes, where each flowsplit is represented by a single volume and every pipe is divided into one or more volumes. These separate volumes are interfaced by boundaries. Scalar variables (pressure, temperature, density internal energy, enthalpy, etc.) are assumed to be uniform over each volume. Vector variables (mass flux, velocity, etc.) are computed at each boundary. This type of discretization grid is referred to as a *staggered grid*, figure 3.4, [5], [20].

The cooling and oil system representations provide predictive models of all components in the circuits including the cooling and oil pumps, thermostats, heat exchangers, pipes, hoses, etc. A fast-running, mean value engine model is utilized.

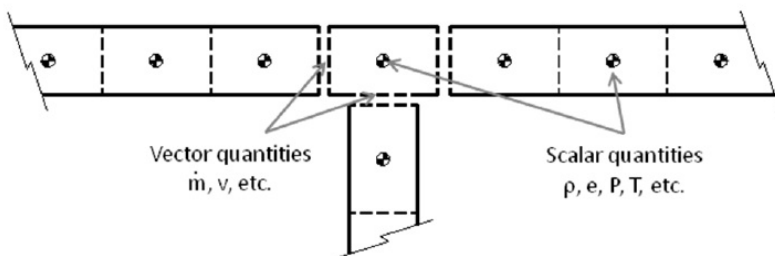


Figure 3.4: Discretization scheme staggered grid for 1D simulation, Courtesy GT-SUITE

## Engine model

The engine model is implemented in GT and coupled to additional engine control blocks (EMS) in Simulink environment. It is a fast running mean value model, which delivers results with satisfactory accuracy and considerable advantages in terms of runtime of the order  $0.5 - 1 \times RT$ . It is based on neural networks<sup>1</sup>, which provide data for volumetric efficiency, IMEP, FMEP, Exhaust temperatures, and NOx levels. It is built as a simplification of a detailed engine model, whose runtime is much longer as it provides detailed models for more physical phenomena.

The input to the engine model is a drive cycle description, which contains time-indexed data for engine torque, speed, vehicle speed and ambient temperature and pressure.

The primary output of interest from the engine model is the instantaneous heat rejection from the burned charge contained in the combustion chamber to the walls of the chamber. This output is routed to a the cooling circuit mode, where the engine block is represented by 5 thermal masses interconnected with thermal resistances [5]. The employed modeling method simplifies the engine block into a single volume for coolant and single volume for oil. The engine structure is represented by 5 thermal masses, figure 3.5. Two of these masses are "inner" that are connected only to one of the fluid volumes and receive direct heat input. The fluid volumes then are connected to the "outer" masses that represent the block, head and crankcase structures. The outer masses can transfer heat with the ambient environment.

## Oil system and temperature dependent model of FMEP

The models of the oil circuit and the temperature dependent model of friction mean effective pressure increase (friction losses) are not yet documented in any publications, but the author chose to include them in this summary, because they are the key link between the effects of engine encapsulation (increased initial engine fluid temperatures) and fuel efficiency.

Engine encapsulation effectively increases the probability for shorter periods of operation

<sup>1</sup>A neural network is an information processing system inspired by the way the human brain works, which implies a parallel computing architecture. NeuralNet components can be used in GT-SUITE control systems anywhere that an output must be determined as a function of one or more inputs. Its basic purpose is therefore similar to that of a simple lookup table or map. However the method by which a neural network calculates its output is quite different. Cited from *GT-SUITE manual* [5]

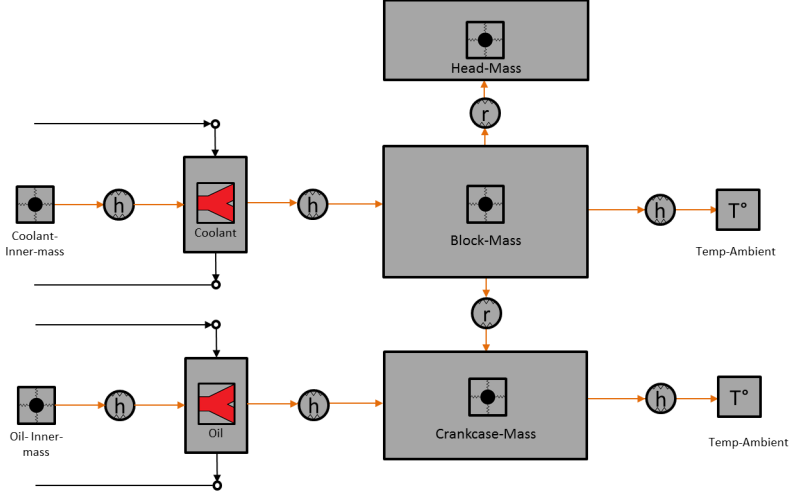


Figure 3.5: 1D thermal model of engine structure represented by 5 thermal masses

under cold oil temperatures, when oil viscosity is high. Therefore a model of the oil system is needed which is capable of predicting oil temperature variation during engine cold start and the resulting effect on FMEP.

The oil system is modeled using the same method as the cooling system. The system includes one water-cooled oil cooler, oil pump, filters thermostatic valve, and a sequence of oil channels and galleries. Performance, dimensional and geometric data are used to create the corresponding models of these components.

The following relationship proposed by Mattarelli [2] was used to capture the effects of varying viscosity on FMEP:

$$FMEP = A + B\sqrt{\mu} \quad (3.1)$$

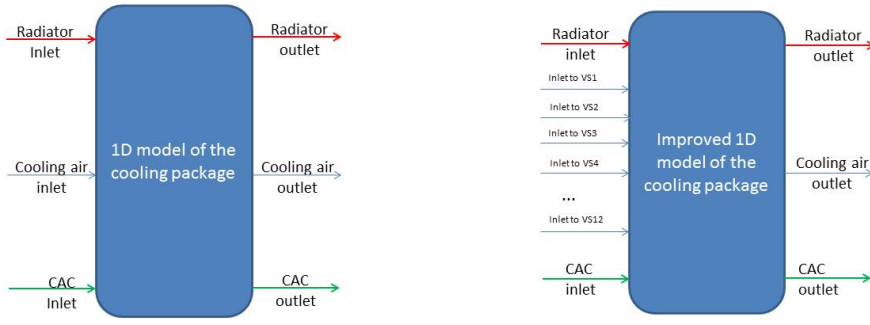
where  $\mu$  is the dynamic viscosity and A and B are constant parameters.

Coefficients A and B are analytically defined and the proposed relationship is implemented in the engine model for below nominal working temperatures of the oil sump.

## 1D representation of flow and temperature non-uniformities

An add-on to GT-SUITE - COOL3D provides an option for quasi-dimensional representation of heat exchangers and their interface with the ambient environment. This allows for a rough discretization of these interfaces and individual application of boundary conditions for each separate section of this discretized interface. This is recommendable for situations where high non-uniformities of temperatures and flow are expected, for example when there are significant flow obstructions in front of the heat exchanger due to the grille or ducting, or high levels of recirculation.

The front face of the charge air-cooler is divided into 12 rectangular sections, which for simplicity will be called virtual sections (VS).



(a) *Uniform boundary conditions*

(b) *Non-uniform boundary conditions*

Figure 3.6

### 3.2.2 3D simulation models

A real size CAD model of complete vehicle in a digital replica of the climatic test wind tunnel with no simplifications was used to generate a computational grid of approx. 65 million polyhedral cells in STAR-CCM+, figure 3.7.

Original CAD geometry was used for generating the mesh pre-processed in ANSA. Heat exchangers are modeled as porous media with characteristics back-calculated from component pressure drop measurements. Heat transfer rates through CAC and Radiator are modeled with NTU effectiveness approach as a result of local flow velocities. Imposed are temperatures and mass flow rates on the inlets of the CAC and radiator, and into the main control volume. [10]

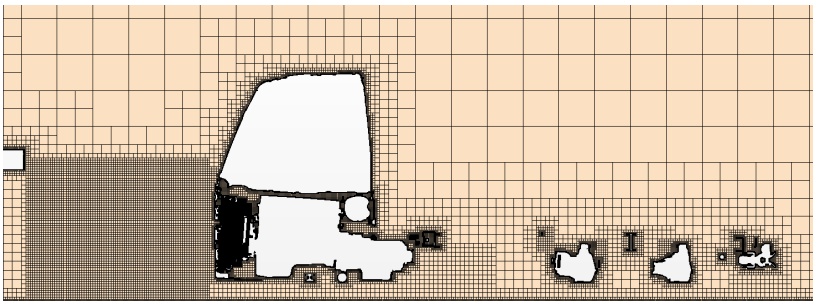


Figure 3.7: *A section cut of the computation grid*

Refinement zones were added in important regions, where better discretization is recommended for accurate flow resolution and heat transfer prediction: in front of the vehicle and in the underhood. Prismatic cells with varying numbers of layers are added at the surface of the vehicle to resolve the viscous sublayer.

Realizable ( $k - \varepsilon$ ) turbulence model is applied to all computational regions in the simulation. The fan is represented by its authentic geometry within a rotating reference frame (MRF).

Boundary conditions from 19 available steady state test runs were imposed and corresponding simulations were performed. Once obtained, the results from the CFD simulations must be analyzed and verified. The main output of interest from the CFD simulation are the local fluid velocities and temperatures extracted from the flow field at the external inlet interface of the charge air cooler.

### 3.2.3 Imposing results from 3D CFD to 1D models

Results for mass flows and mass-averaged temperature levels are extracted from the CFD solution of the flow field for regions specified to correspond to the respective virtual sections from the 1D representation. Thus exact quantifications of mass flows and mass-averaged temperatures per virtual section are acquired for each simulation run. Figure 5 shows mass flow variation through one virtual section presented as a function of fan speed and vehicle speed. Presented are 19 different results – one from each simulation.

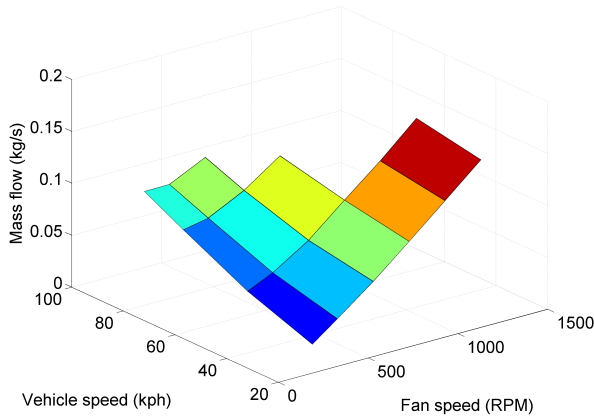


Figure 3.8: *Variation of mass flow for one virtual section*

A central design question at this stage is how to effectively impose the results from the steady state 3D simulations onto the 1D model of the cooling package. A correctly implemented approach would preserve the predictive nature of the solution of the flow dynamics in the 1D model. This requirement precludes the option to directly impose quantities for mass flow and temperature. Instead, it has been decided to add a certain amount of pressure loss to each virtual section in the 1D model until the respective mass flow rates match data from CFD. This is achieved by the use of 12 pressure loss objects in parallel, directly connected to each virtual section. Thus, the number of inlet air connections to the model of the cooling package increase. See figure 3.6b.

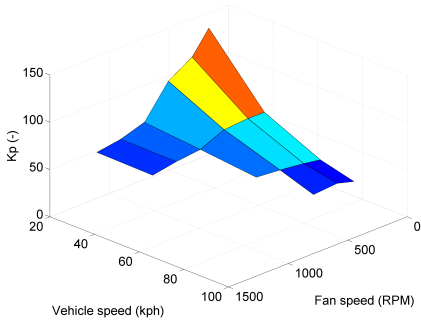
The pressure loss objects impose a flow-dependent pressure increase computed as

follows:

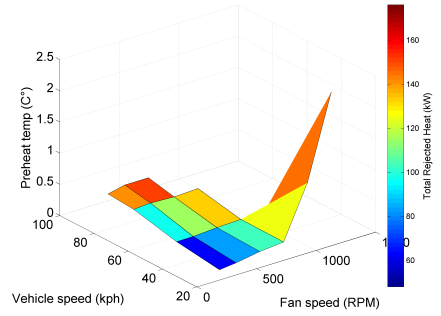
$$\Delta P = \frac{1}{2} K_p \left( \frac{\dot{m}}{\rho A_{ref}} \right)^2 \quad (3.2)$$

The resulting pressure loss coefficients for each virtual section are plotted against fan speed and vehicle speed. Figure 3.9a.

A similar method is employed to capture the mass-averaged temperature increase over the ambient level. It is based on a hypothesis that temperature rise as a result of recirculation can be mapped with sufficient accuracy as a function of vehicle speed, fan speed and total rejected heat through the cooling package. Figure 3.9b visualizes this. This is a calibration procedure and requires test data or comprehensive 3D simulations performed with a validated method.



(a) Variation of pressure loss coefficient for one virtual section



(b) Variation of mass-averaged inlet air temperature increase due to recirculation as a function of vehicle speed, fan speed and total rejected heat.

Figure 3.9

## 4 Results

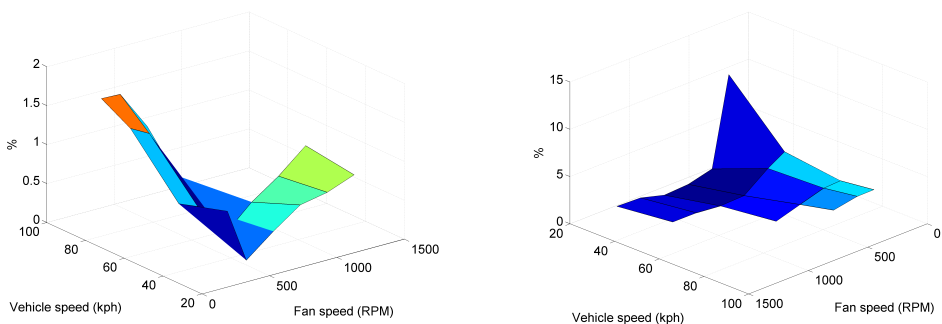
### 4.1 Results from basic 1D model

The main aim with this model is to establish and validate a simulation platform, which is capable to simulate continuous unsteady drive cycles and by use of a detailed 1D representation of the cooling system, including coolant circuit and air path, provide outputs for any physical property or quantity in the coolant and oil circuits.

Presented are results from a simulation, which utilizes the method described in section 3.2.1 and in Paper A [14], but the test vehicle used for these simulations is different. The following simulation is carried out for an 13L FM distribution truck. Therefore the results can be treated as an additional level of method validation to the one presented in the above-referenced paper.

#### 4.1.1 Steady state simulations

Calibration of this model is performed by tuning an overall pressure loss coefficient (accounting for pressure loss in engine bay) and overall mass-averaged increase in ambient temperature to capture the effect of recirculation. Inputs for this calibration are measurements from tests. The results on figure 4.1 present the difference between the measured and simulated temperatures on the outlet of the hot media normalized with the inlet temperature difference. The inlet temperature difference is defined as the difference between the temperatures of the hot inlet stream and the cold inlet stream into the core of the heat exchanger.



(a) Radiator outlet temperature. Magnitude of simulation inaccuracy expressed as a percentage of inlet temperature difference. Model without non-uniformity

(b) CAC outlet temperature. Magnitude of simulation inaccuracy expressed as a percentage of inlet temperature difference. Model without non-uniformity

Figure 4.1

### 4.1.2 Continuous transient drive cycle simulations

Presented are predictions for a number of physical properties of interest to cooling system analysts including radiator inlet temperature, CAC outlet temperature, fan speed, coolant mass-flow rate, etc.

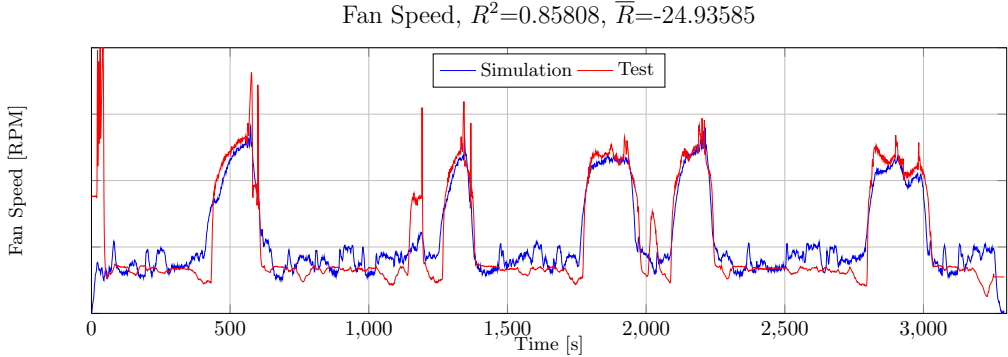


Figure 4.2: Plot: Fan speed

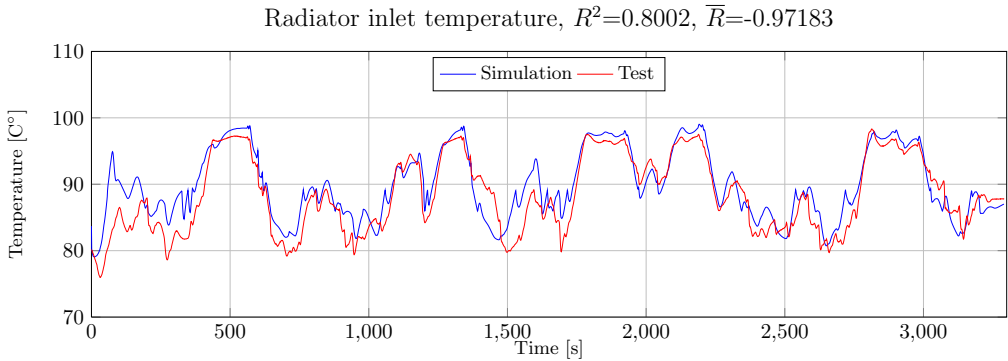


Figure 4.3: Plot: Radiator inlet temperature

High levels of consistency between simulated values (in blue) and measured values (in red) are achieved. High coefficient of determination  $R^2$  are obtained for most parameters of interest. The relatively low values for  $R^2$  shown on figure 4.4 are due to an imperfection of the coolant pump control strategy, which switches the mode of pump operation too early at approx.  $t = 1400s$  and at  $t = 2300s$ . This erratic behavior of the control system influences the simulated values for radiator coolant temperature during the periods of misprediction.

Figure 4.6 shows satisfactory consistency between the inlet charge air temperatures from test and simulation.

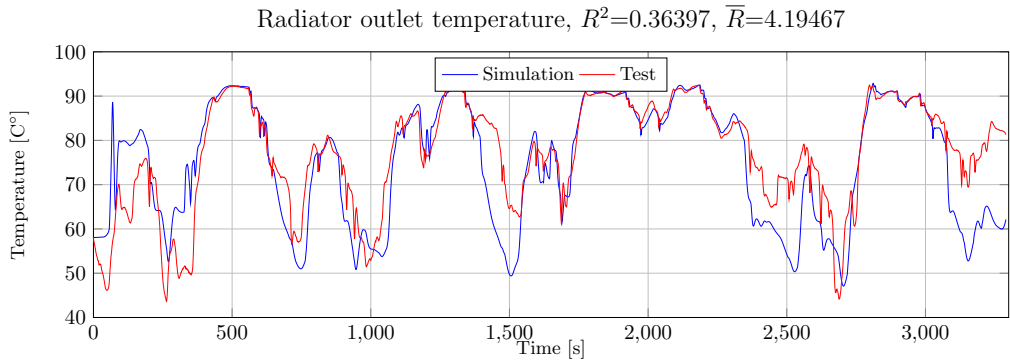


Figure 4.4: Plot: Radiator outlet temperature

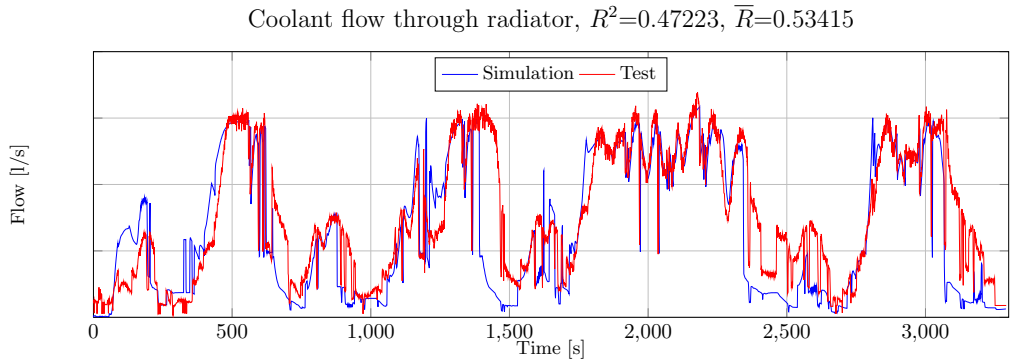


Figure 4.5: Plot: Coolant flow through radiator

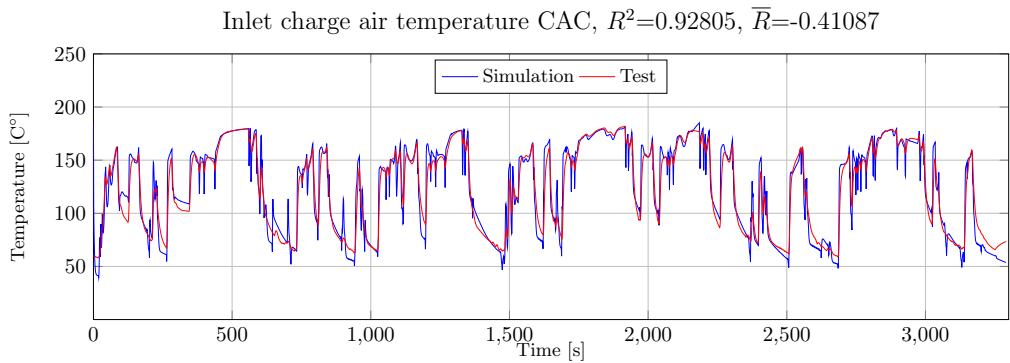


Figure 4.6: Plot: CAC inlet temperature

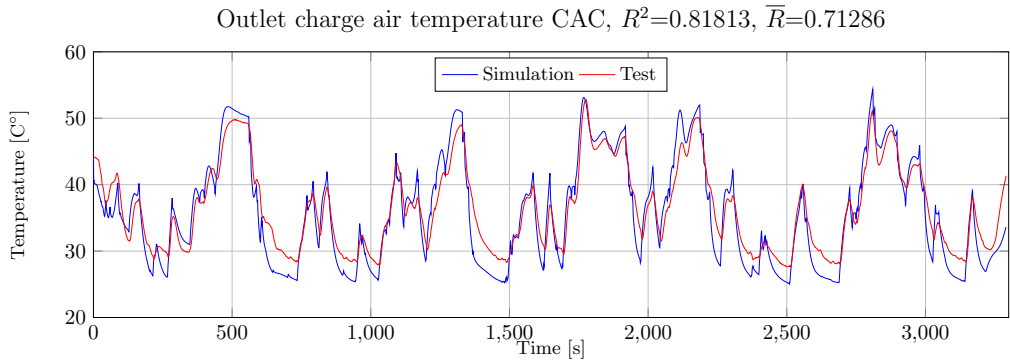


Figure 4.7: Plot: CAC outlet temperature

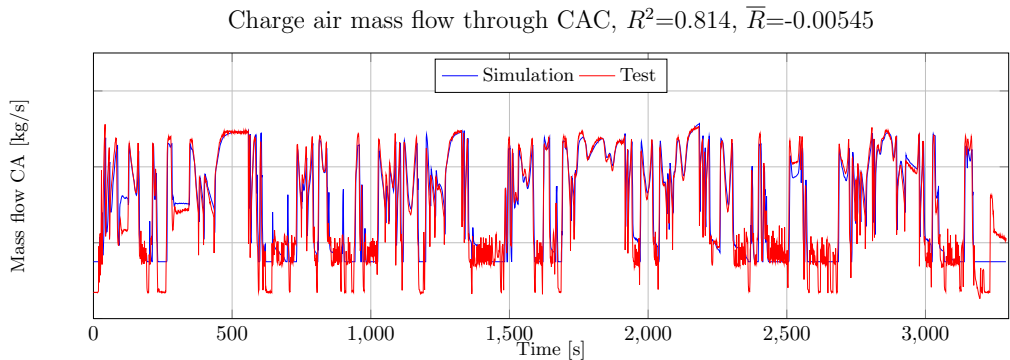


Figure 4.8: Plot: Mass flow CAC

## 4.2 Results from 3D simulations of complete vehicle

Nineteen steady state simulations were performed to replicate test measurements from a dynamometer wind tunnel. Measured values for vehicle speed, fan speed, radiator inlet temperature and mass flow, CAC inlet temperature and mass flow are imposed as boundary conditions to the model. The computations were performed on 200 cores. Most cases converged within less than 3000 iterations and 3 hours (600 CPU hours). A representation of the temperature field in a central section plane, parallel to the longitudinal axis of the vehicle, is shown on figure 4.9. The non-uniform mass-flow and temperature distribution through the cooling package are shown on figures 4.10a and 4.10b.

The results on figures 4.9, 4.10a and 4.10b are from a simulation at 25 km/h vehicle speed, full fan engagement – 1200 RPM, and ambient temperature of 25  $C^\circ$ .

The validation strategy for the CFD simulations is to compare temperatures on the outlet of the heat exchangers from measurements with simulation results. The simulation

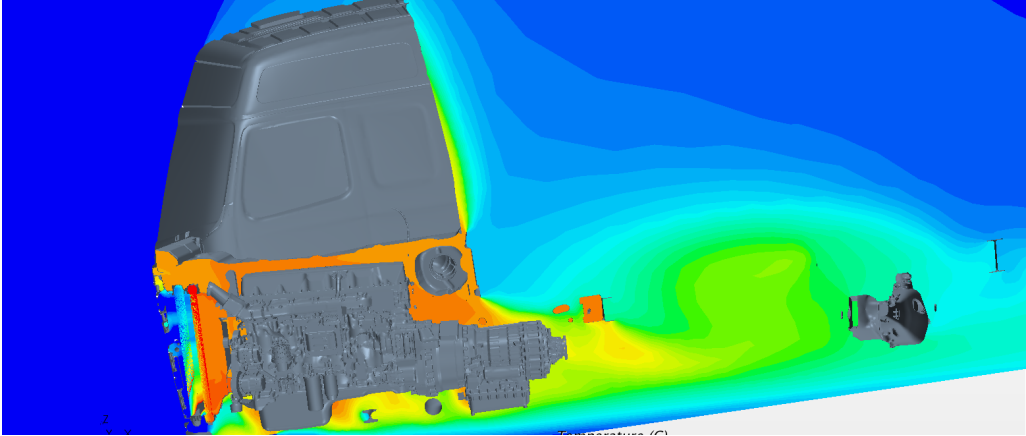
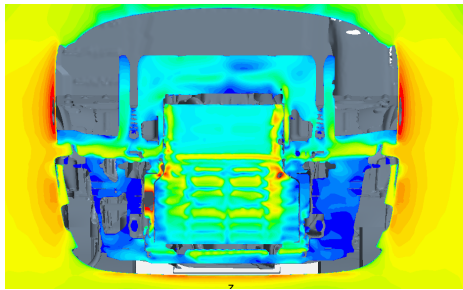
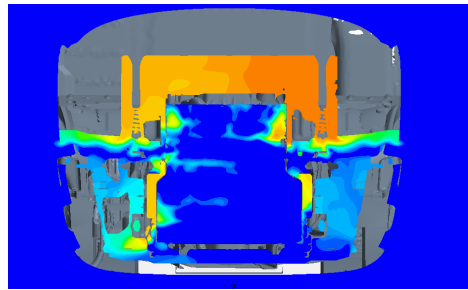


Figure 4.9: *Temperature field through underhood*



(a) *Distribution of velocity of cooling air through inlet plane of CAC*



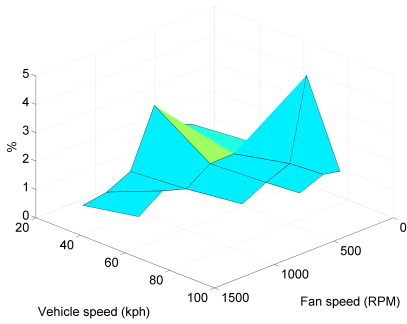
(b) *Distribution of temperature of cooling air through inlet plane of CAC*

Figure 4.10

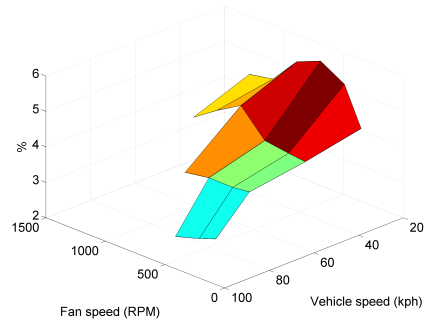
method is considered trustworthy as long as the inaccuracy is within 5% of the inlet temperature difference per heat exchanger.

Average error of less than 2% is observed for the computed radiator outlet temperature. Figure 4.11a. Higher, but permissible inaccuracy is reported for the simulated CAC outlet temperature. Most of the simulation runs of high inaccuracy are at low ram-air speed, where recirculation is prominent. Recirculation is a phenomenon primarily driven by the fan. The effects of recirculation increase with increasing fan speeds. High fan speeds are usually present at low vehicle speeds, where the ram air alone is not sufficient to propel enough mass flow through the underhood. Therefore recirculation has its highest magnitude at low road speeds and high fan speeds. Furthermore, recirculation is a strongly 3-dimensional phenomenon, which requires comprehensive turbulent models and high grid resolution to be captured realistically.

The accuracy of the 3D simulation model is considered high for the internal industrial standards and practices and is seen as sufficient for the purposes of this analysis.



(a) Radiator outlet temperature. Magnitude of simulation inaccuracy expressed as a percentage of inlet temperature difference. CFD results compared with test measurements.

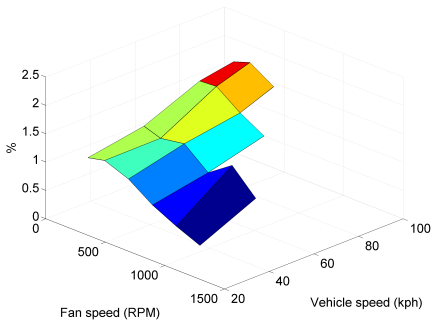


(b) CAC outlet temperature. Magnitude of simulation inaccuracy expressed as a percentage of inlet temperature difference. CFD results compared with test measurements.

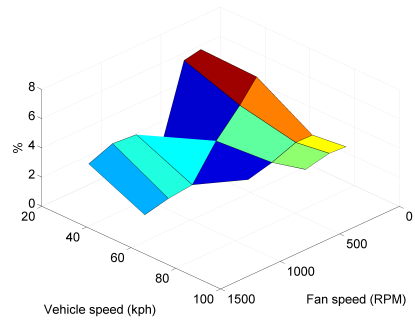
Figure 4.11

### 4.3 Results from a 1D model with non-uniform boundary conditions with input from 3D simulations

Values for temperature and mass-flow distribution are extracted from the 3D CFD solution and are imposed on an uncalibrated 1D model as explained in section 3.2.3. The resulting accuracy, figures 4.12a and 4.12b, is comparable with the results achieved by direct calibration using results from tests.



(a) Radiator outlet temperature. Magnitude of simulation inaccuracy expressed as a percentage of inlet temperature difference. Model with non-uniformity.



(b) CAC outlet temperature. Magnitude of simulation inaccuracy expressed as a percentage of inlet temperature difference. Model with non-uniformity.

Figure 4.12

For the selected discretization (number of virtual sections) and number of performed

experiments, there is no indication that imposing non-uniform boundary conditions from CFD results, onto a 1D model of a cooling package improves simulation accuracy. The approach with uniform boundary conditions, figures 4.1a and 4.1b, provides comparable magnitudes of error.

However the benefits of the latter approach are seen in the proven integration between 3D and 1D simulation tools. Calibrations of 1D model of a cooling system are successfully performed by use of a validated 3D CFD method.

## 4.4 Unsteady simulations of engine cold start and predictions of fuel consumption

The models of engine, cooling and lubrication systems have been coupled as described in section 3.2.1 to allow for analysis of fuel consumption as a result of variations in initial engine oil temperature. Available are measurements from a standard test of engine cold start. Engine speed and torque for this drive cycle are shown in figure 4.13.

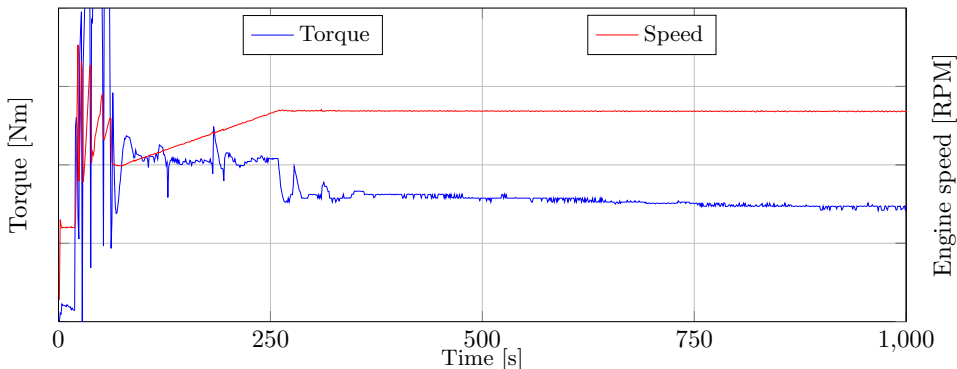


Figure 4.13: Plot: Engine speed and torque during cold start cycle

Predictions for temperature of coolant and oil are produced by the 1D coupled model, figures 4.14 and 4.15.

The accuracy of the presented results is considered sufficient for the purposes of this model. Figure 4.14 shows a short delay in the simulated temperature rise after  $t = 500$ s. This slower time response is attributed to the time response characteristics of the thermostat model and its capacity coefficients at closed state. Nevertheless, the steady state error is negligible.

The simulated development of engine oil temperature in the oil sump is shown on figure 4.15. The initial parabolic shape of the measured temperature is a direct consequence of the behavior of viscosity, which decreases with temperature. In addition to this, the magnitude of heat flux between the engine internals and the lubricant is proportional to the their temperature difference. As oil viscosity decreases during the warm up cycle less mechanical energy is converted into heat. Furthermore, the temperature difference

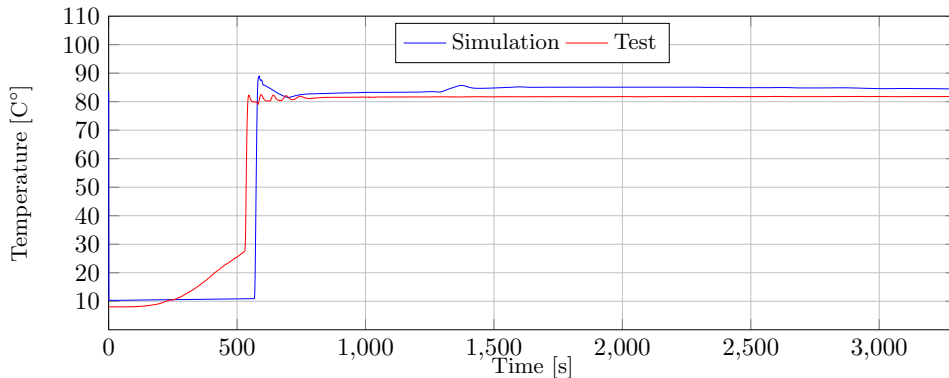


Figure 4.14: *Plot:Radiator inlet temperature during cold start cycle*

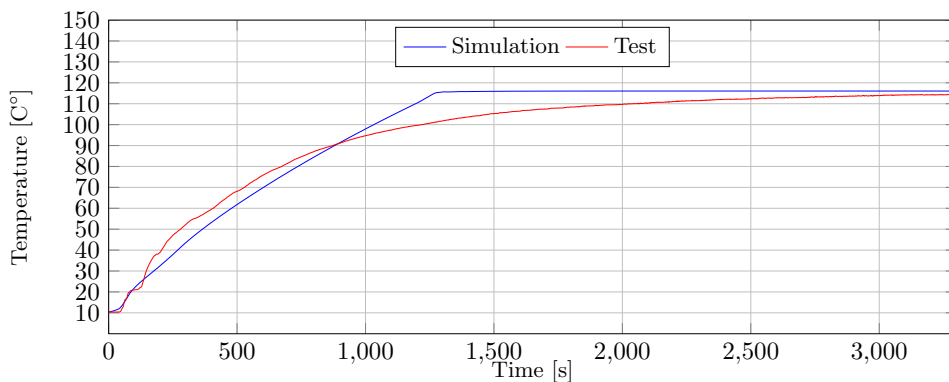


Figure 4.15: *Plot: Temperature in oil sump during cold start cycle*

between the internal engine surfaces and the engine oil itself will decrease as the cycle progresses. Both these effects result in initially high and continuously decreasing heat flux into the oil. This interesting trend in the development of oil temperature is captured and plotted. Here it must be noted that the simulated values are for mass-averaged temperature in the oil sump, while the corresponding physical measurement is local.

The advantage of using a predictive engine model directly integrated in the simulation is used to obtain a reading for instantaneous fuel consumption. A comparison between computed and measured fuel consumption for the same cold start drive cycle is shown on figure 4.16.

The presented results show an outstanding agreement between measured and simulated fuel mass flow, which is obtained entirely analytically. Of greatest interest to this research is the amount of burned fuel in the beginning of the simulation, when the effects of high oil viscosity on FMEP are most pronounced. For purposes of clarity a magnification of this part of the cycle is given on figure 4.17:

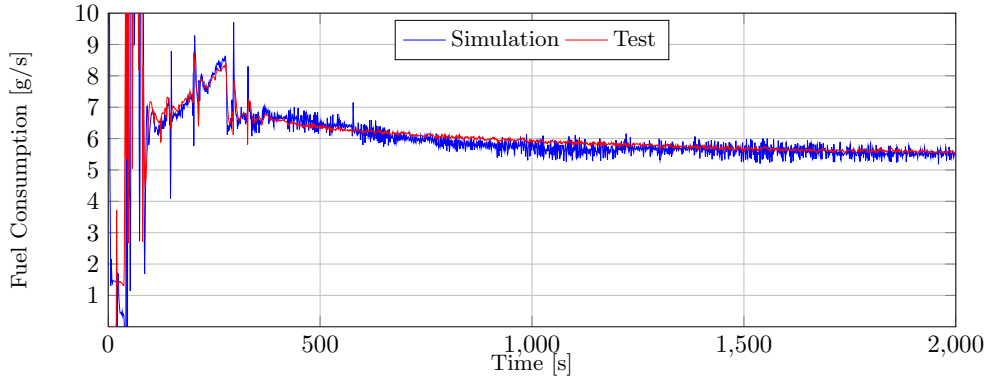


Figure 4.16: *Plot: Instantaneous fuel consumption during cold start cycle: measured vs. computed results*

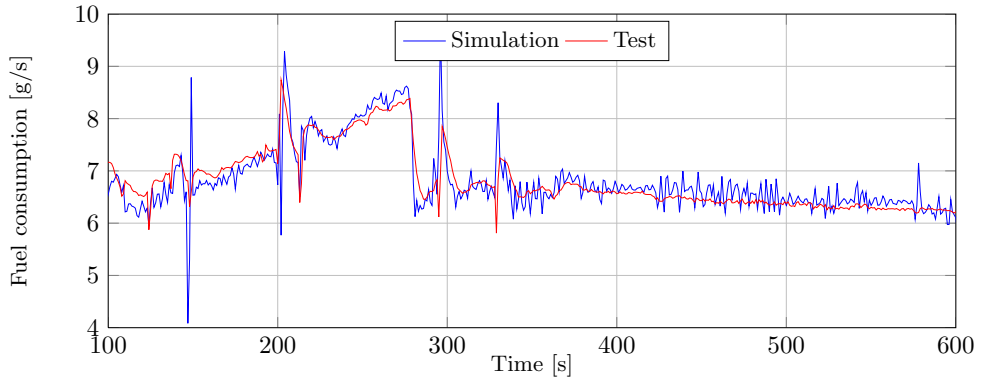


Figure 4.17: *Plot: Instantaneous fuel consumption during cold start cycle: measured vs. computed results*

A simulation of the same drive cycle is performed, but with high initial temperatures of engine oil and coolant. Both engine fluids and all thermal masses have been preset to an initial value of  $T = 70C^\circ$ . Results for computed fuel consumption are shown on figure 4.18:

Figure 4.18 shows a significant difference between the readings for fuel consumption at different initial oil temperatures. A time integration of the obtained values for fuel consumption of the initial warm-up period would give the total amount of fuel consumed. This is done for a series of experiments performed for a number of initial engine temperatures in the range of 10 to 90  $C^\circ$ , figures 4.19 and 4.20.

The employed method reported a potential for up to 3% reduction of fuel consumption during engine warm up.

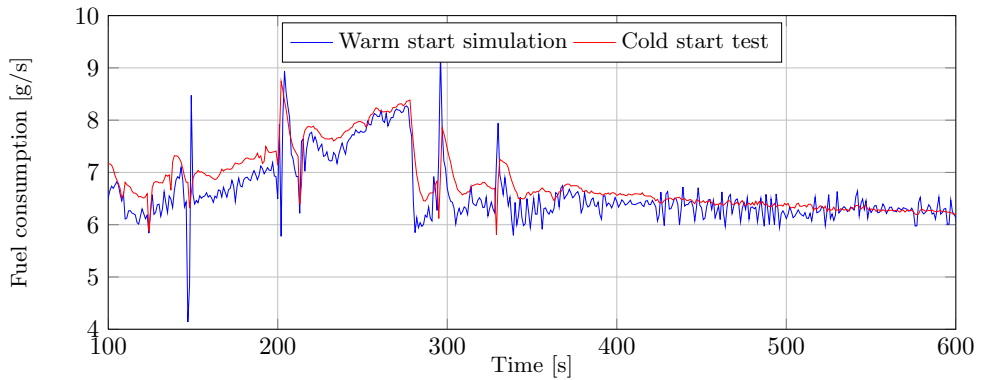


Figure 4.18: Plot: Computed fuel consumption during hot engine start compared to measured fuel consumption during cold engine start

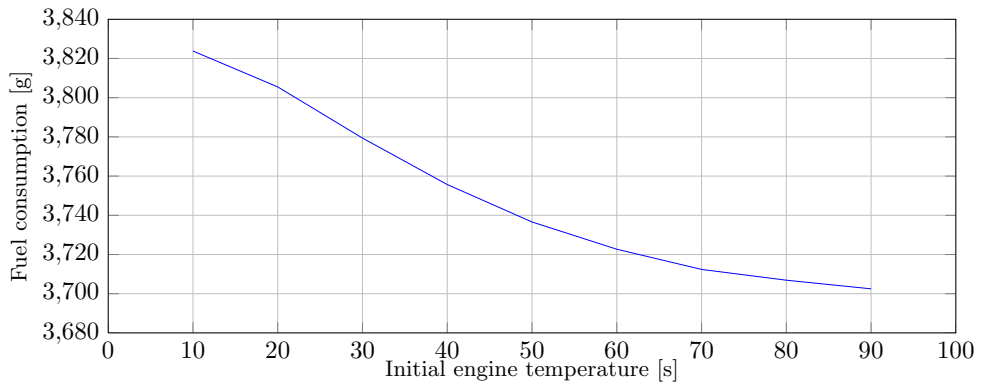


Figure 4.19: Plot: Variation of total fuel consumption during warm-up for different initial oil temperatures

The benefits of thermal engine encapsulation increase with the frequency of cold starts in the operational cycle of the vehicle. Passenger vehicles used for short-distance urban driving, but also distribution vehicles operating in cold ambients can profit from an engine encapsulation concept, whose immediate effect is to reduce heat transfer from engine to ambient.

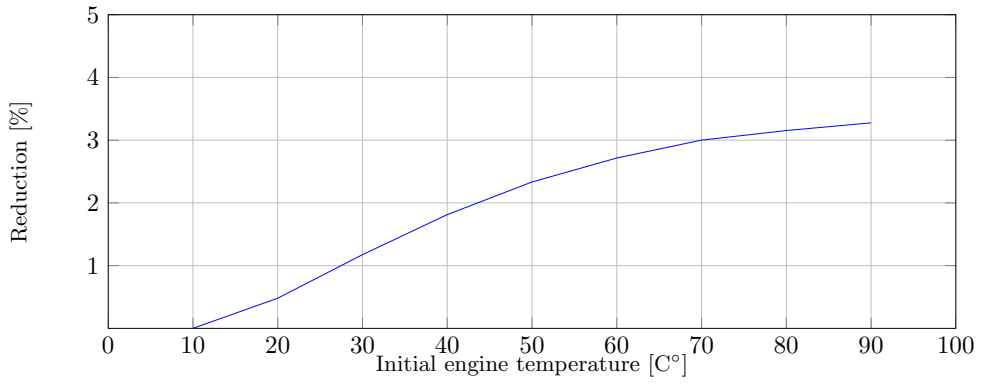


Figure 4.20: *Plot:Reduction of fuel consumption as a result of initial oil temperature*

## 5 Conclusions

Presented is a 1D unsteady model verified against experimental data and supported with parallel 3D simulations. It contains predictive models of engine, cooling system, oil circuit and utilizes a temperature dependent model of engine friction losses. The 1D transient model has been validated by comparison of simulated results with measurements from a dynamometer test. Satisfactory consistency between computed and measured readings for coolant and oil temperatures were reported.

Results from 3D CFD simulations were used to calibrate a 1D model of the cooling system with non-uniform temperature and flow boundary definition on the inlet of the cooling package. The implementation of the non-uniform boundary strategy did not result in any measurable increase in simulation accuracy, but the analysis confirmed that validated 3D CFD methods can be used to calibrate 1D models of the underhood air path with excellent results in the absence of data from physical measurements.

Models of the engine, cooling and oil systems were coupled with a temperature dependent engine friction model. A series of complete vehicle simulations of a cold start drive cycle at different initial oil temperatures were performed in order to evaluate the influence of reduced warm-up phase on fuel consumption.

The simulations indicated up to approx. 3% decrease in fuel consumption as a result of reduced initial oil viscosity for the simulated drive cycle. This percentage is expected to vary depending on the specific drive cycle, but it is still considered a sufficient motivation for implementing engine encapsulation in applications with high frequency of engine cold starts.

## 6 Future work

It is intended to continue using the results, conclusions and tools developed in this work for future studies of engine encapsulation and simulations of specific encapsulation concepts. Development of additional comprehensive models of complex phenomena in the engine underhood is intended to further improve the capabilities and the accuracy of the presented simulation platform, figure 3.2.

The most immediate enhancement planned for near future is a 3D transient model of natural convection in the engine bay, which would allow to predict the varying rate of heat release and temperature drop of engine fluids after shutoff.

Additionally planned enhancements of the presented model include studies of the effects of radiation in the engine bay.

# References

- [1] C. Adapco. StarCCM+ Manual, 9.02.005 edition (2014).
- [2] A.Muscio and E.Mattarelli. Potential of Thermal Engine Encapsulation on Automotive Diesel Engines (2005). DOI: 2005-24-067.
- [3] Y. A. Cengel, R. H. Turner, and J. M. Cimbala. *Fundamentals of Thermal-Fluid Sciences*. McGraw Hill, 2008. ISBN: 978-007-126631-4.
- [4] F. Fortunato et al. Underhood Cooling Simulation for Development of New Vehicles (2005). DOI: 2005-01-2046.
- [5] *GT-SUITE Flow Theory Manual Version 7.3*. Gamma Technologies. 2012.
- [6] J. B. Heywood. *Internal Combustion Engine Fundamentals*. McGraw Hill International Editions, 1988.
- [7] K. Holmberg and P. Andersson. Global energy consumption due to friction in trucks and busses. *Tribology International* **13.78** (2014), 94-114.
- [8] W.-H. Hucho. *Aerodynamics of road vehicles*. Society of Automotive Engineers, 1998.
- [9] S. Kaushik. Thermal Management of a Vehicle's Underhood and Underbody Using Appropriate Math-Based Analytical Tools and Methodologies (2007). DOI: 2007-01-1395.
- [10] L. Larsson. Investigation of Rear-Mounted Cooling Module Installations for Heavy Vehicles (2011).
- [11] K. Mahmoud, E. Loibner, and J. Krammer. Integrated 1-D Tools for Modeling Vehicle Thermal Management System (2004). DOI: 2004-01-3406.
- [12] D. M. Mantovani et al. Innovative concepts for thermo-acoustic engine compartment encapsulation (2010). URL: [www.rieter.com](http://www.rieter.com).
- [13] *MATLAB manual. Ordinary Differential Equations*. Version 7.8. Mathworks, 2008. URL: <http://www.mathworks.com/access/helpdesk/help/techdoc/ref/ode45.html>.
- [14] B. Minovski and L. Löfdahl. Study of Software Integration for Transient Simulation of Future Cooling System for Heavy Truck Application (2014). DOI: 10.4271/2014-01-0653.
- [15] B. Minovski, L. Löfdahl, and P. Gullberg. A 1D Method for Transient Simulations of Cooling Systems with Non-Uniform Temperature and Flow Boundaries extracted from a 3D CFD solution (2015).
- [16] B. Petroleum. BP Statistical Review of World Energy June 2014 (2014). URL: <http://www.bp.com/statisticalreview>.
- [17] Redrawing the energy-climate map. *OECD/IEA International Energy Agency* (2013).
- [18] B. Rosenau. Multifunctional Encapsulations of the Power Train (2003).
- [19] F. Storckenmaier, M. Brinkammer, and V.Caldiero. Multifunctional Encapsulations of the Power Train (2006). DOI: 2006-01-1234.
- [20] H. K. Versteeg and W. Malalasekera. *An Introduction to Computational Fluid Dynamics*. Prentice Hall, 2007. ISBN: 978-0-13-127498-3.